

Petr Bour¹
Jan Kubelka²
Timothy A. Keiderling²
¹ Institute of Organic
Chemistry and Biochemistry,
Academy of Sciences
of the Czech Republic,
Flemingovo nám. 2, 16610,
Praha 6, Czech Republic

² Department of Chemistry
(M/C 111),
University of Illinois
at Chicago,
845 W. Taylor Street,
Chicago, Illinois 60607-7061,
USA

Received 23 July 1999;
accepted 29 October 1999

Simulations of Oligopeptide Vibrational CD: Effects of Isotopic Labeling

Abstract: Simulated *ir* absorption and vibrational CD (VCD) spectra of four alanine-based octapeptides, each having its main chain constrained to a different secondary structure conformation, were analyzed and compared with experimental results for several different peptides. The octapeptide simulations were based on transfer of property tensors from a series of *ab initio* calculations for a short *L*-alanine based segment containing 3 peptide bonds with relative ϕ , ψ angles fixed to those appropriate for α -helix, 3_{10} -helix, ProII-like helix, and β -sheet-like strand. The tripeptide force field (FF) and atomic polar tensors were obtained with density functional theory techniques at the BPW91/6-31G** level and the atomic axial tensor at the mixed BPW91/6-31G**/HF/6-31G level. Allowing for frequency correction due to the FF limitations, the octapeptide results obtained are qualitatively consistent with experimental observations for *ir* and VCD spectra of polypeptides and oligopeptides in established conformations. In all cases, the correct VCD sign patterns for the amide I and II bands were predicted, but the intensities did have some variation from the experimental patterns. Predicted VCD changes upon deuteration of either the peptide or side-chains as well as for ¹³C isotopic labeling of the amide C=O at specific sites in the peptide chain were computed for analysis of experimental observations. A combination of theoretical modeling with experimental data for labeled compounds leads both to enhanced resolution of component transitions and added conformational applicability of the VCD spectra. © 2000 John Wiley & Sons, Inc. Biopoly 53: 380–395, 2000

Keywords: oligopeptide; vibrational CD; isotope labeling; *ir* absorption; theoretical simulation

Correspondence to: Timothy A. Keiderling; tak@uic.edu
Contract grant sponsor: Grant Agency of the Czech Republic (CR) and NIH
Contract grant number: 203/97/P002 (CR) and CGM30147 (NIH)
Biopolymers, Vol. 53, 380–395 (2000)
© 2000 John Wiley & Sons, Inc.

INTRODUCTION

In recent years the use of ir techniques for conformational analysis of peptides and proteins has expanded dramatically.¹ In particular, the frequencies and relative intensities of the components forming the amide transitions have traditionally proven to be the most diagnostic characteristics for determining the average fractional secondary structure contents in proteins.^{2–4} In ir absorption, relative frequencies have been the most utilized spectral feature because the band shapes are not as variable as are found with differential spectral techniques, such as CD, which are normally analyzed with band shape techniques.^{5–7} This has resulted in analyses dependent on empirical rules for assignment of characteristic frequencies corresponding to different secondary structure types, especially for the amide I band (composed primarily of the C=O stretch on the amide linkage).^{2,3} Various researchers have demonstrated that this approach is too simplistic and leads to nonunique solutions.^{4,8–10} As a simple example, while it is very well known that α -helices absorb at $\sim 1650\text{ cm}^{-1}$ for proteins in D₂O, α -helical poly-L-lysine¹¹ and the highly α -helical alanine-rich peptides based on (AAAAK) repeats^{10,12,13} absorb below 1640 cm^{-1} . Recent quantum-chemical-based force field (FF) calculations have demonstrated that even ideal, but finite α -helices have spectral components spread over the whole usual amide I region.^{14,15} Nonetheless, these empirical, frequency-based relationships provide a useful means of characterizing at least the dominant secondary structure type in many systems. That they lack a sound theoretical base is a challenge left to stimulate the development of improved theoretical methods.

We have promoted the use of vibrational CD (VCD) as an improved sensitivity diagnostic for secondary structure type because it is a naturally differential technique where analysis is dependent on band shape and has only a secondary dependence on frequency shifts of the component bands.^{7,16–19} Examples are known where a common secondary structure type, such as an α -helix, gives rise to a conserved VCD bandshape but one shifted to different frequencies in different peptides.^{12,20–22} In analogy to band shape based ir studies^{23–26} and to well-established electronic CD studies,^{5,6,27–30} we have in the past developed empirical correlations of amide I and II^{31–33} and even amide III³⁴ VCD band shapes with secondary structure.

For small molecule systems, VCD band shapes and spectra can be simulated with very satisfying accuracy using ab initio quantum mechanical force fields and similarly computed atomic polar and axial tensors

(APT and AAT, respectively), the latter typically obtained with what is sometimes referred to as the magnetic field perturbation (MFP) method.^{35–39} Very good results can often be obtained with the MFP method by use of the density functional theory (DFT) approximation for introducing a partial correction for configuration interaction thereby improving the computed vibrational frequencies and consequently the appropriateness of the FF and normal modes from which the VCD is simulated.^{39–47} At the present time, the large size of oligo- and polypeptides needed to attain a well-defined dominant secondary structure, and thus are commonly studied experimentally, usually prohibits direct simulation of their VCD with ab initio quantum mechanical methods. However, we have already shown that even an approximate calculation, at the HF/4-31G level for a pseudo-dipeptide constrained to ϕ , ψ dihedral angles characteristic of selected secondary structure types, can yield simulated VCD band shapes in qualitative agreement with the experimental results.⁴⁸

Recently Bour et al.⁴⁹ have developed a technique for transfer of the atomic polar tensors (APT) and atomic axial tensors (AAT) parameters from an ab initio calculation on a smaller molecule to align with the structure of a larger molecule that encompasses the smaller one as a fragment. These transferred APT and AAT values can then be used with the normal modes resulting from a similarly transferred FF parameters to produce simulated ir and VCD spectra. In our initial study,⁴⁹ the method was tested by computing the VCD of a glycine-based pseudo-tripeptide and comparing it with results obtained using transferred tensors from a pseudo-dipeptide. Subsequently, the VCD of an α -helical heptapeptide was simulated from calculations for a pseudo-tripeptide, where none of these pseudo-peptide molecules were configurationally chiral nor had real side chains (other than hydrogen). Nevertheless, those calculations were very promising and suggested that the method might usefully describe characteristic VCD for different secondary structures (VCD spectra of α -helices in the amide I have always been the easiest to reproduce with any level of theory). If the method gave realistic spectral band shapes for different secondary structures and for other bands and could be adjusted to reproduce the proper frequencies, it would be a logical next step to extend the method to simulate the VCD of mixed secondary structures and, eventually, of proteins. This paper reports the first step in that direction, simulation of the VCD and ir spectra of an octapeptide composed of L-alanine residues and constrained to the ϕ , ψ dihedral angles characteristic of four common secondary structure types, α -helix, 3_{10} -helix,

poly-L-proline II (ProII-like) helix, and a β -sheet-like strand.

Recently, Fourier transform ir (FTIR) spectra of isotopically labeled peptides and proteins have appeared in the literature.^{50–55} These observations demonstrate that isotopic substitution can enhance resolution of vibrational spectra and provide a means of locally probing the peptide conformation in a site-specific manner. As will be shown, an advantage of the methods used in this study is that natural and isotopically labeled peptides can be modeled consistently. Moreover, the isotopic substitution leads to negligible additional computational cost in terms of required computer CPU time.

METHOD

Peptide force fields and electric tensors for larger peptides were obtained using a method of transferring their Cartesian components from small peptides that we have described recently in detail.^{49,56} The model tripeptide (with respect to the number of amide groups) used for the basis (small molecule) ab initio MFP calculations consists of two L-alanine residues N-terminated with an acetyl group and C-terminated with a methyl amide to form a total of three amide bonds, yielding a formula structure: $\text{CH}_3\text{—CONH—CH}(\text{CH}_3)\text{—CONH—CH}(\text{CH}_3)\text{—CONH—CH}_3$. This “pseudo-alanine-tripeptide” molecule was used as a source of the force field and atomic tensors that were transferred to the larger oligopeptides studied. The structure mimics a segment of a poly-L-alanine peptid chain and is analogous to the simpler “pseudo-dipeptide,” $\text{CH}_3\text{—CONH—CH}_2\text{—CONH—CH}_3$, which we originally used to simulate the local contributions to peptide VCD spectra for different secondary structure conformations.⁴⁸ Thus the present model, which explicitly incorporates chiral α -carbons (on the L-Ala residues) and a “1–3” amide–amide interaction, should better represent vibrational properties of common peptide chains. Vibrational interactions are dominated by local, mechanical through-bond coupling so that such a tripeptide model should provide the most important contributions to the force field. We presume that the tripeptide model even better describes the atomic polar and axial tensors, properties that are assigned only to single atoms, but which are consequences of the bonding and stereochemistry about that atom. Hydrogen bonding, transition dipole coupling, and solvent effects could not be included in these calculations, in part due to limitations of our computational resources. Our previous simulations⁵⁷ of the spectral impact of hydrogen bonding and solvent interactions imply that their effect on VCD spectra should be limited.*

* Test calculations⁵⁸ on N-methyl acetamide (NMA) with two hydrogen-bound waters in an Onsager reaction field show a decrease in the amide I and amide II band frequency separation to about 135 cm^{-1} from 215 cm^{-1} for NMA in vacuo. Such a large computed change is actually consistent with changes in the NMA amide I and II frequencies seen between vapor phase⁵⁹ and con-

Table I List of the Peptide Torsion Angles, Kept Constant for the Four Conformations of the Trimer and Used for Octamer Construction^a

| | Conformation | ω | ψ | ϕ |
|-------|-----------------|----------|--------|--------|
| H, H8 | α -helix | 180 | –47 | –57 |
| E, E8 | β -sheet | 180 | 124 | –128 |
| G, G8 | 3_{10} -helix | 180 | –30 | –60 |
| P, P8 | Polyproline II | 180 | 149 | –78 |

^a Torsional angles for β -sheet conformation are the averages of parallel and antiparallel β -sheet (for further explanation see text)⁴⁸; all other angles are standard.⁶⁹

Neglect of dipole coupling may indeed be a more serious approximation. Miyazawa⁶² developed a general perturbation model and Krimm and co-workers^{14,63–66} and more recently Mendelsohn⁶⁷ have used it to show that transition dipole coupling, particularly between strands, can lead to large effects in the β -sheet normal modes. These effects are much less significant for α -helices. The impact on the corresponding VCD parameters is unknown and is left to a future study. Its inclusion involves adding empirical parameters to an a priori force field that would then lead to an imbalanced theoretical treatment.⁶⁸

The geometry of the model tripeptide was optimized using constraints on the peptide main chain ϕ , ψ torsion angles. All peptide bonds were set to be planar and *trans*, $\omega = 180^\circ$. Four conformations were simulated: right-handed α -helix and 3_{10} -helix, left handed poly-L-proline II (ProII or 3-1)-like helix, and an extended β -sheet-like strand, which corresponds to the most common peptide conformations previously studied with VCD.[†] The conformational parameters used are summarized in Table I.

For the geometry optimization and force field determination, the Gaussian 94 program package⁷⁰ was used to compute second derivatives of the energy using DFT methods with the BPW91 DFT functional and a standard 6-31G** basis set.^{71,72} APT and analytical second derivatives of the energy which form the harmonic FF were obtained for the optimized tripeptide geometries at this same level of approximation. For the local part⁴⁹ of the AAT, which are needed for VCD simulation,^{35–39} the HF/6-31G level AAT values were used as obtained from calculations with the CADPAC program package.⁷³ The distributed origin gauge was used for the tripeptide, as we and others have previously done for smaller molecules.^{39–47}

The local AAT parameters were then combined with APT and FF tensors obtained from each of the DFT calculations and transferred to a model “alanine-octapeptide,”

densified phases.^{60,61} Even at this reduced separation, the normal mode coupling does not seem to have a significant effect on the calculated dipole derivatives.

[†] The ϕ , ψ values for a β -sheet-like strand are taken as an average of those for antiparallel and parallel β -sheet,⁶⁹ since no major spectral differences between these two types are experimentally established.⁴⁸

Table II Calculated Amide I Frequencies, and Dipole and Rotational Strengths for the Octapeptide in Four Conformations^a

| Mode | H8 (α) | | | E8 (β) | | | G8 (3_{10}) | | | P8 (ProII) | | |
|------|-----------------|-----|-----|----------------|-----|-----|-----------------|-----|-----|------------|-----|------|
| | ν | D | R | ν | D | R | ν | D | R | ν | D | R |
| 1 | 1744 | 64 | -37 | 1728 | 28 | -3 | 1735 | 45 | -32 | 1736 | 16 | 10 |
| 2 | 1740 | 110 | -62 | 1726 | 37 | -3 | 1730 | 34 | -29 | 1734 | 4 | -8 |
| 3 | 1739 | 26 | -26 | 1723 | 5 | -6 | 1729 | 32 | -13 | 1733 | 4 | 19 |
| 4 | 1736 | 40 | -4 | 1717 | 13 | 4 | 1728 | 70 | -23 | 1731 | 6 | -48 |
| 5 | 1731 | 68 | 61 | 1712 | 1 | -4 | 1726 | 111 | -11 | 1728 | 42 | 273 |
| 6 | 1725 | 14 | 46 | 1707 | 14 | 2 | 1721 | 42 | 69 | 1725 | 152 | 60 |
| 7 | 1718 | 10 | 1 | 1704 | 6 | -5 | 1715 | 9 | 14 | 1722 | 65 | -247 |
| 8 | 1713 | 15 | 8 | 1703 | 274 | 2 | 1708 | 37 | 10 | 1720 | 2 | -14 |

^a ν in cm^{-1} , D in 10^{-3} Debye², R in 10^{-7} Debye². Note: in the cgs system both D and R have the same unit ($\text{esu}^2 \text{cm}^2$); therefore we use the atomic unit Debye² for both (in SI based atomic units the R unit is Debye-Bohr magneton). This commonality of units relates to the experimental measurement of A and ΔA having the same units.

$\text{CH}_3\text{—CO—}[\text{NH—CH}(\text{CH}_3)\text{—CO}]_7\text{—NH—CH}_3$. Geometry parameters to constrain the octapeptide to the four secondary structure types considered were the same as used for the tripeptide species as specified in Table I, resulting in four longer peptides which we refer to as H8, G8, P8, and E8 for α -, 3_{10} - and ProII-helix and β -sheet conformations. A set of programs written in-house enabled us to introduce various isotopic substitutions, compute the vibrational frequencies and normal modes (diagonalize the FF), and combine them with the APT and AAT parameters to calculate the ir and VCD spectra of these systems.⁴⁹ Theoretical spectra were simulated using Lorentzian band shapes with band widths of 20 cm^{-1} (FWHM) for each component, which results in an approximate correspondence to experimentally observed spectral characteristics.

Our experimental evidence indicates that VCD spectra of regular structures of this length have virtually the same band shapes (although in some cases a bit broader) and most of the intensity per residue as found for a polypeptide of the same conformation.^{7,74–77} The effect of length on the frequencies is perhaps also interesting,^{24,78} but the ab initio frequencies computed with the DFT FF are in general much further from the experimental values than could be accounted for by length dependence alone. In summary, we view the shapes, as evidenced by sign patterns and relative intensities, to be the primary test characteristics that determine the value of this simulation exercise.

Calculated rotational (R) and dipolar (D) strengths were obtained by transfer of APT and AAT values from the tripeptide to the octapeptide structure using the techniques previously described in detail.⁴⁹ From these octapeptide D and R values the theoretical spectra were also simulated using Lorentzians as was done for the tripeptides.

Apart from the inaccuracy stemming from the BPW91/6-31G** approximation, we attribute the main errors in calculated parameters to neglect of solvent and hydrogen bonding, neglect of transition dipole coupling and use of the harmonic approximation. Previously, only limited effects of the use of different approximation levels for computing the

AAT^{79–81} were observed in terms of the overall accuracy of simulated VCD spectra for selected small molecules. We also expect that alternate treatments of the VCD simulation, such as the vibronic coupling theory (VCT)⁸² model, may give similar accuracy but could have different basis set sensitivity, a characteristic that might be probed in a future study with expanded computational resources.

RESULTS AND DISCUSSION

Calculated spectra for oligomers create a huge number of transitions, most of whose component bands are heavily overlapped with other transitions arising from combinations of equivalent local modes. In judging the efficacy of the calculations, simulated spectral band shapes, whereby each component is given a realistic line width and summed to give the resultant spectrum, are much more efficient than endless tables of ν , D , and R values. Such full tables are available from the authors on request. As an example of the pattern resulting from the coupling of eight local modes, the amide I mode values are listed in Table II for the octapeptide in the four structures studied. These tables give an idea of the distribution of intensity in both D and R , over the bands normally associated with the amide I that have a large component of amide C=O stretching motion. It becomes clear, as has been noted previously,^{14,15} that the bands have significant dispersion ($20\text{--}30 \text{ cm}^{-1}$), even without inclusion of perturbation due to H bonds or dipole coupling, which speaks to the difficulty (and even illegitimacy) in assigning a given frequency to a single secondary structure type.^{4,8,9} What becomes clear is that a shift of the major intensity distribution among the components is responsible for much of the char-

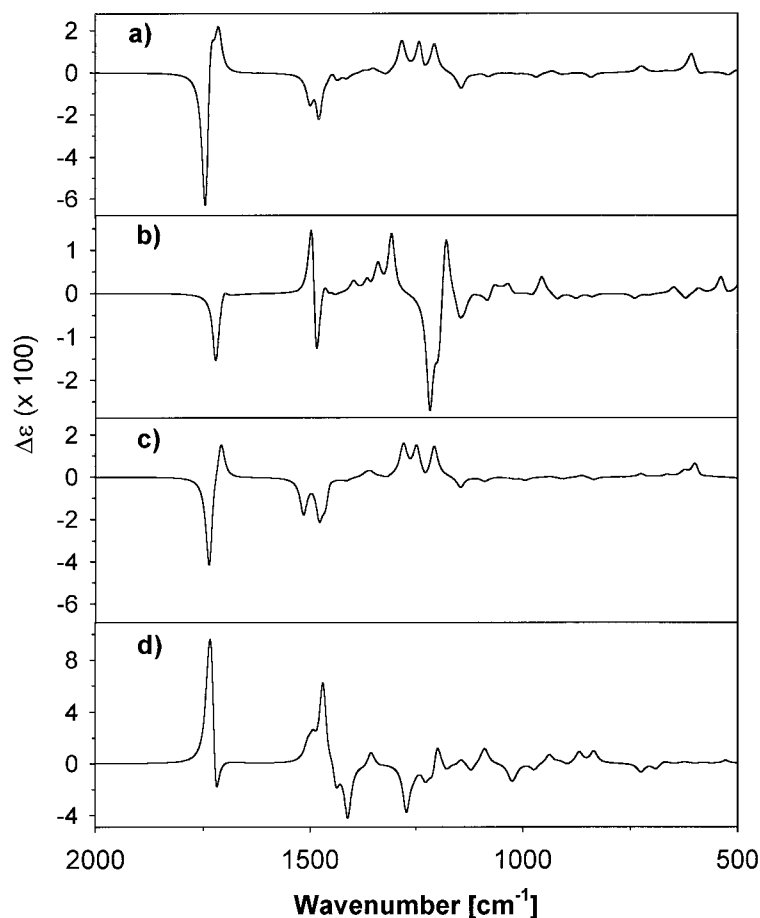


FIGURE 1 Simulated VCD spectra for the model alanine tripeptide in (a) α -helix, (b) β -sheet, (c) 3_{10} -helix, and (d) ProII helix conformations (calculations at the BPW91/6-31G**/HF/6-31G level).

acteristic secondary structure frequency response. For example, for the α -helix amide I, the higher frequency components have the higher D values for the 8 amide I components, while for the sheet and ProII simulations the lower frequency components are relatively more intense. Thus while the E8 and G8 amide I frequency distributions are both lower than that of H8, the intense G8 component is more than 20 cm^{-1} higher than the intense E8 component. In addition, the maximal R and D values do not occur for the same component in a given conformation, which might be expected from the dependence of R on the magnetic dipole contribution to the transition moment, and leads to frequency shifts between dominant ir and VCD bands.

Tripeptide

Ab initio, DFT BPW91/6-31G** (for FF and APT)/HF/6-31G (for AAT) simulated VCD spectra over much of the mid-ir region for the tripeptide in the four

conformations (Table I) are illustrated in Figure 1. The spectral shapes approximately correspond to the results we previously obtained for just the dipeptide model in these same conformations.⁴⁸ The amide I couplets for the α -helix and ProII conformations are less conservative than for the dipeptide and evidence distinct splittings, and the 3_{10} couplet is more realistic than for the dipeptide in shape, but not in intensity. Linear Ala tripeptides normally do not have a stable structure, so a direct comparison of these (Figure 1) results with experimental data for the molecules calculated is not sensible. However, if the VCD is indeed accurately modeled by primarily local interactions, as implied by our oligopeptide length dependent experimental data,^{7,74–76} then comparison of these calculated tripeptide spectra to experimental results for longer oligopeptides and polypeptides is a reasonable test of whether this empirically established near-neighbor property is evidenced in the calculations. That was the procedure used in the previous dipeptide paper⁴⁸; thus the comparisons discussed here reflect

that same approach. Generally, the amide I tripeptide computed VCD results are again in qualitative agreement with experimental spectra having the correct sign pattern (positive couplet for both the α -helix and 3_{10} -helix, negative couplet for the ProII helix, and weak but net negative VCD for β -sheet; note the scale changes for β -sheet and ProII simulations).^{7,12,48,74–77,83–85} However, at least in the ProII case, there is qualitative disagreement with experiment in terms of the relative intensity of positive and negative lobes (experimentally the negative lobe is more intense). The intensities relative to the amide II are also more problematic, especially for 3_{10} -helix.

As might be expected, greater differences between the tripeptide (Ala-like) and dipeptide (Gly-like) simulated spectra can be found for the amide II modes that are naturally more affected by the bonding configuration on the α -carbon, and apparently in these calculations, by overlap with the Ala local CH_3 deformation modes. The tripeptide calculation predicts an overall negative amide II signal for α - and 3_{10} -helices, in accordance with experimental spectra,^{85–87} but more structure (splitting) and much less relative intensity (for 3_{10}) are computed than seen experimentally. On the other hand, the amide II band for the ProII-like model, obtained as a weak negative for the dipeptide, becomes highly split, which again is probably an effect of mixing with the CH_3 modes.

Vibrational frequencies for the amide I and amide II modes obtained directly from this DFT BPW91/6-31G** force field are closer to experimental values as compared to those obtained from the unscaled HF/4-31G FF used for the previous dipeptide computations,⁴⁸ as is expected for DFT vs. HF results.^{36–44} However, those earlier dipeptide calculations were scaled before the published figures were prepared, so the difference is not immediately evident. The DFT frequencies presented here are used without any scaling. The amide II frequencies are in closer agreement with the experimental values, being low by only 10–30 cm^{-1} , while calculated frequencies for the amide I are about 80–100 cm^{-1} high. This results in amide I–II separation being about 100 cm^{-1} too large, a difference from experiment that can be attributed fundamentally to FF error coupled with the neglect of solvent and hydrogen bonding in our simulations. Since such overestimations are also seen in N-methylacetamide DFT calculations,⁵⁸ this is unlikely to be due to neglect of dipole coupling. Overestimation of the amide I–II splitting may be an important factor influencing the ultimate accuracy and applicability of these simulations since it will necessarily underestimate the coupling of local motions contributing to both modes. Addition of anharmonic interactions, hy-

drogen bonds, and explicit solvent effects is beyond our available computational resources for tripeptide DFT calculations. This is certainly an area for future work, especially given the impact of hydrogen bonding on the frequency separation.⁵⁸ One potential empirical correction would be to transform the coordinates to allow scaling of the amide I (C=O stretch) to get a more accurate splitting for comparison to experimental spectra and more realistic mixing of local amide I and II type motions. (However, in a preliminary test for the amide I of peptides with coordinates of the α -helix, no significant change in the predicted VCD band shape or intensity was found when scaling the C=O FF to get reasonable amide I and II frequencies.⁸⁸) Similar difficulties in accurately calculating nonamide C=O stretching frequencies with DFT FF methods were observed in some previous VCD studies of small molecules.^{44,45} Even worse amide I and II frequencies are found with the other popular density functional, B3LYP, often used for vibrational simulations.^{49,88,89}

Thus, for the conformationally most important amide I and II modes, we can conclude that the computed spectra for the tripeptide (Ala) model are substantially consistent with the previous dipeptide (Gly) results, the biggest impact being the Ala side chain interference with the amide II vibrational modes. These interferences are eliminated if one does a computation with substitution of $-\text{CD}_3$ side chains (results not shown, see below). The amide III modes are also encompassed in the spectra shown in Figure 1 ($\sim 1200\text{--}1300\text{ cm}^{-1}$). These are, as is consistent with experimental observations,³⁴ very weak in intensity and moreover are heavily overlapped with what appear to be side-chain modes, making them much less easy to compare to experiment. It is interesting that the spectral region that encompasses the amide III is net positive for α -helix and net negative for β -sheet, in qualitative agreement with our recent experimental results.³⁴ Transitions at lower frequencies were computed, of course, and as seen in Figure 1, are generally weaker than even the amide III bands. Since no systematic experimental results are yet available for these lower energy bands, they will not be addressed further. However, these tripeptide simulations suggest that, given the right solvent system, samples with longer path lengths (to compensate for the low dipole and rotational strengths without having to drastically increase concentration) could yield measurable VCD for these as yet unexplored transitions.

Octapeptide

Simulated octapeptide IR and VCD spectra for the four conformations as obtained with transferred FF,

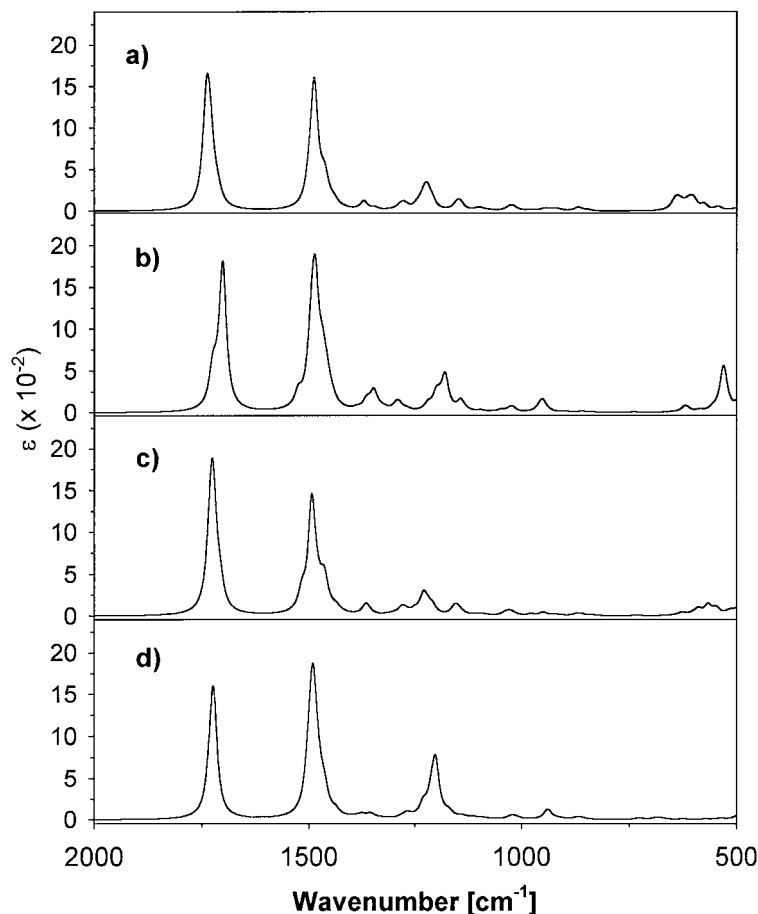


FIGURE 2 Simulated ir absorption for the model alanine octapeptide in (a) α -helix, (b) β -sheet, (c) 3_{10} -helix, and (d) ProII helix conformations obtained by transferring the FF and APT tensors from the tripeptide determined as in Figure 1.

APT, and AAT parameters are shown in Figures 2 and 3, respectively, the latter providing a direct comparison to those of the tripeptide in Figure 1. The ir bands show intense amide I and II bands that are split by more than 200 cm^{-1} , twice as large as seen experimentally. The main amide I peak for the β sheet strand is substantially lower in frequency and more split than the other conformers, as noted earlier and as detailed in Table II, but is still far short of the observed experimental splitting. However, the amide II ir intensities, relative to those of the amide I, are uniformly larger than observed experimentally for all the conformations.

Most of the changes seen for the amide I and II VCD intensities in going from tripeptide to octapeptide simulations improve the agreement of simulated spectra with experimental results. The amide I couplets for the ProII, α -, and 3_{10} -helices all become more conservative (Figure 3, positive and negative lobes more in balance), and the detailed splittings

seen for the tripeptide simulations (Figure 1) get smoothed out with the contributions from 8 transitions overlapping. The relative intensities of the octapeptide ProII and β -sheet amide I vs amide II VCD bands also become more reflective of the experimental amide I:II intensity ratios. The VCD amide I magnitudes, in terms of $\Delta A/A$, are $>10^{-4}$ for α -helix and ProII helix, and are much weaker for β -sheets, also as seen experimentally. These changes do not affect the basic sign pattern determined by the short-range amide–amide interaction already present in the tripeptide.

This apparent convergence of spectral properties suggests that the octapeptide is long enough to provide a model-limited simulation of VCD band shape features for peptide chains of arbitrary lengths. In other words, going to, for example, 16 residues is unlikely to change the band shape much at this level of theory. For comparison, experimental VCD data for several peptides with these characteristic second-

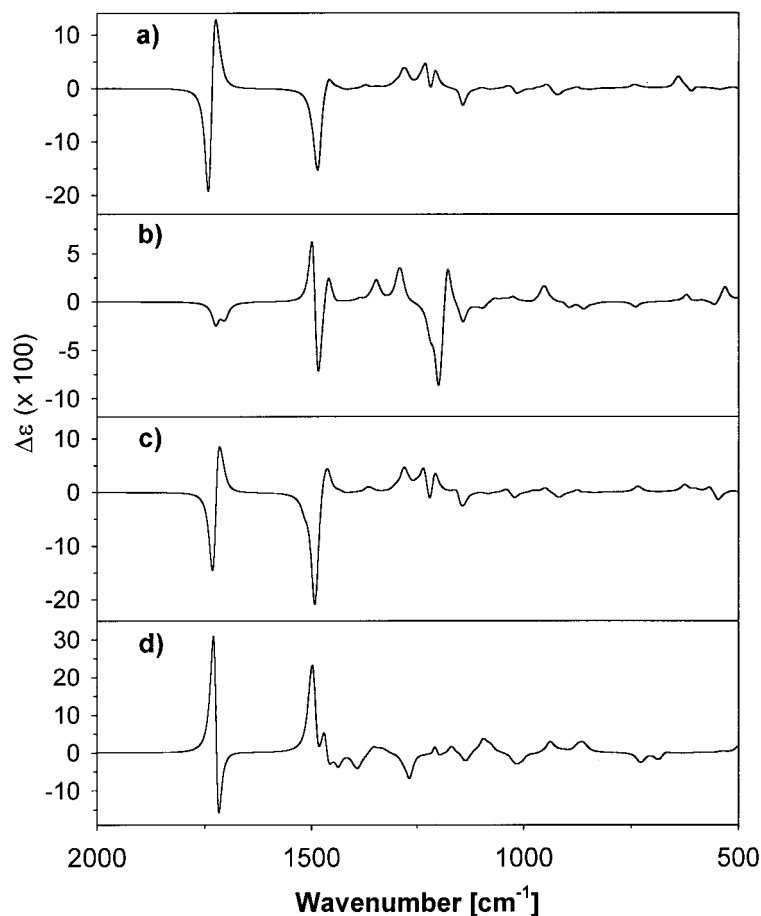


FIGURE 3 Simulated VCD spectra for the model alanine octapeptide in (a) α -helix, (b) β -sheet, (c) 3_{10} -helix, and (d) ProII helix conformations by transferring FF, APT, and AAT parameters from the results for the tripeptide (Figure 1).

ary structures are shown in Figure 4. The qualitative agreement of the various simulations with the fundamental character of the VCD band shapes is evident.

The amide III modes continue to be dispersed with side chain modes in the octapeptide simulations, having a net positive for α -helix and net negative for β -sheet, in agreement with experimental results. We have also simulated the amide A (N—H stretch) VCD and found it to have a negative couplet shape for both the α - and 3_{10} -helix conformations, in agreement with early experimental observations.^{85,90,91} The simulated amide A VCD for β -sheet (negative) and ProII helix (positive) are computed to have a single sign, which is a very unusual VCD pattern for high dipole moment transitions. However, these conformations lack good comparative experimental data in the amide A band to confirm or refute such predictions.

Comparison of the β -sheet form of the peptide chain with experiment is quite problematic, since β -sheets in real systems are composed of multiple

hydrogen-bonded β -strands. Experimentally, the absorption band for β -structures splits into a higher frequency shoulder or minor peak (as high as 1690 cm^{-1} for an antiparallel aggregate peptide) and a dominant lower-frequency band ($<1630\text{ cm}^{-1}$). This splitting is dependent on peptide length, uniformity, and on the interstrand H-bond and transition dipole interaction.^{63,92,93} These interstrand interactions could not be accounted for in our ab initio tripeptide calculation, where only a single strand, with typical “ β -sheet” torsional angles could be modeled. As can be seen in Figure 2 this characteristic splitting is only suggested in our a priori computed simple β -strand octapeptide ir spectra, and is significantly underestimated as compared to the experimental results for anti-parallel sheets. Krimm and co-workers⁶³ have demonstrated that by use of transition dipole coupling with Miyazawa’s perturbation formulas,⁶² a better representation of the splitting for β -sheets can be found. At present this is an empirical correction that

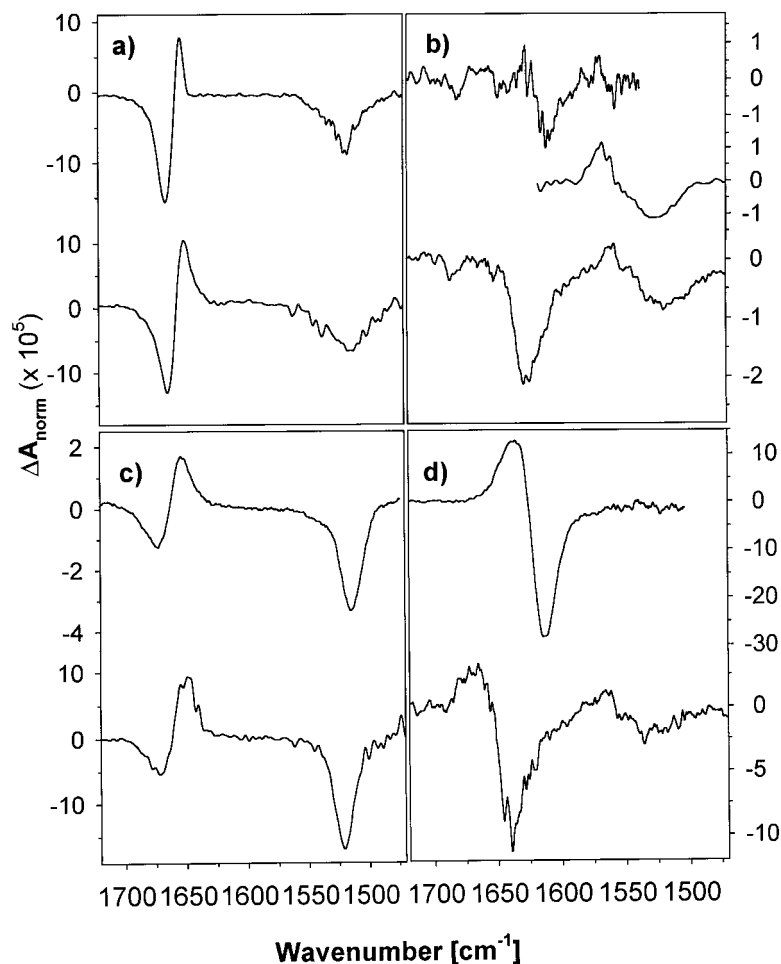


FIGURE 4 Experimental VCD for comparison to the computed VCD in Figure 3 for (a) α -helix: poly- γ -benzyl-L-Glu (top), $(\text{Met}_2\text{-Leu})_6$ (bottom); (b) β -sheet: (Lys-Leu) polymer under high salt conditions (amide I'—top), poly-L-Lys at high pH and high temperature conditions (amide II—middle), Immunoglobulin G (bottom); (c) 3_{10} -helix: $(\alpha\text{-Me-Val})_8$ (top), $\text{Aib}_2\text{-L-Leu-Aib}_5$ (bottom); and (d) ProII helix: $(\text{Pro})_{12}$ (amide I'—top), poly-L-Lys (bottom).

must be added to the force field as an adjustable parameter.^{67,68} A priori simulation of the peptide in a more complete, multiple strand, β -sheet conformation should be done first, including intra- and interstrand interactions, before adding empirical corrections. Computations for a relatively large two-stranded oligopeptide fragment would be very complex at the ab initio level and for now must be left to the future.

The relatively low β -sheet amide I frequency as compared to other secondary structure types is qualitatively reproduced in our calculations, showing that this characteristic of β -sheets is due to the ϕ , ψ conformational character and not solely to H-bond strengths as has been often suggested. Moreover, the nature of each of the normal modes can be investigated, by plotting the dynamic displacements for the

lowest and highest frequency amide I modes for the β -sheet octapeptide. The direction of the transition dipole moment resulting from these motions for the higher frequency amide I modes is approximately parallel to the β -sheet strand axis while that for the lower frequency, more intense (dipolar, ir) modes is approximately perpendicular to the peptide strand axis. This exactly follows well-established ir polarization properties for β -sheet polypeptides⁹³ with the intensity centered on the band components at the extremes of the frequency in contrast to the helical cases where the intensity is more clustered in a few, close-lying components.

As for VCD, the β -sheet example also has a different distribution of rotational strengths (R), as compared to the helical patterns (Table II). The β -sheet R

values are all uniformly very small and sum to a negative value. However, the most intense (ir) band component, the lowest frequency one, actually creates a positive VCD contribution resulting in a shift of the maximum negative VCD intensity from the ir peak. Such patterns have been seen experimentally, evidenced as band shape distortions, but the positive distortion may also occur on the higher frequency side of the band. By contrast, the helical patterns have 2 or more intense (high R value) modes that are opposite in sign. In ProII-like helices they tend to alternate with increasing frequency, with two very large but overlapping transitions yielding the negative couplet, while for the α - and 3_{10} -helices, the higher frequency modes tend to be negative and the lower frequency ones positive, leading to a positive couplet. The unusual nature of the β -sheet results suggested that twist of the sheet might be important. Therefore, we carried out two additional calculations by adding a twist of about 10° per residue, one right and the other left-handed in sense, to the extended sheet-like conformation. These twists caused no significant changes in the relative intensity distribution from that shown in Figure 3 for the amide II and III bands as well as those lower in energy. However, the amide I VCD did change a bit. While remaining overall net negative, the right-twisted strand is computed to have an amide I VCD with two negative bands (lower frequency component more intense) but the left-twisted has a positive couplet corresponding to the lower frequency absorption component, which would make the apparent VCD higher in frequency than the absorbance maximum. We have measured such β -sheet VCD for selected oligopeptides in solution.⁹⁴ The overall lack of well-defined ϕ , ψ angles for the β -sheet conformation and the shallowness of this region in a Ramachandran map suggest that this is an unsettled problem. Eventually it may be necessary to simulate β -sheet VCD by averaging results for an ensemble of conformations.

N—H Deuteration

Deuterated solvents, particularly D_2O , are often used for VCD experiments for the convenience of reducing interfering absorptions. For peptides and most proteins this leads to an H/D exchange of the amide N—H bonds to a degree of completeness determined by the fold pattern. Experimentally, complete exchange results in a shift of the amide II down in frequency by $\sim 100\text{ cm}^{-1}$. The VCD pattern of the amide I (now termed I') is not affected very much by N-deuteration, except for the α -helix case where the N—H positive couplet pattern (+, -, low to high)

becomes a 3-featured (-, +, -) band shape for N—D. Isotopic substitution is easily modeled in the harmonic approximation since same force field, atomic axial, and atomic polar tensors can be used as for the unsubstituted molecule. Only the masses need to be altered before the normal mode computation.

Simulated VCD spectra of the N-deuterated octapeptides are plotted in Figure 5. While the amide I vibrational frequency is not significantly changed by the deuteration, only a $\sim 5\text{ cm}^{-1}$ shift was computed (note this is without hydrogen bonds, i.e., these changes are only due to differences in local mode mixing), the amide II frequency does shift down substantially, $\sim 80\text{ cm}^{-1}$, to become the amide II' in accord with experimental observations. The amide I' VCD band shapes are qualitatively the same as for the undeuterated case, but the intensities change somewhat. The 3_{10} amide I' is much weaker than the amide II' VCD, that of the ProII becomes more positive, and the β -sheet loses its splitting and consequently becomes more negative (relative peak intensity). The characteristic 3-peak amide I' VCD for α -helices was not seen in these calculations, implying it may depend on hydrogen-bond interactions (internal to the helix). The amide II' VCD is in some cases obscured by overlap with the CH_3 deformations, which consequently makes its VCD band shape hard to interpret, but overall the amide II' VCD has the same sign pattern as does the amide II.

Deuteration of Side Chains, $CH_3 \rightarrow CD_3$

In order to clarify the influence of the alanine side-chain vibrations on the computed VCD spectra, we "perturbed" the sequence by deuteration of the methyl groups in the octapeptide. The simulated spectra computed for the four conformations, with isotopically induced shifting of interfering side-chain vibrations, are shown in Figure 6. These spectra provide the most clear comparison to the experimental amide I and II spectra (Figure 4) where, in fact, the side chains, make little contribution.^{7,16,95} Presumably in real heteropolymers, the side chains might be expected to contribute little to the VCD, due to their variation in the sequence and to the variety of geometries available to their flexible open chains. By contrast, in our calculations all the side groups are $-CH_3$ and are rigidly repeated (uniform conformation), which can lead to artificially enhanced coupling compared to that found for heteropolymers with rotating side chains. These CD_3 -based computed spectra are also closest in band shape and nature to those presented in our original work⁴⁸ for the dipeptide model system where we employed pseudo atoms (of mass 30 or 15) to mimic

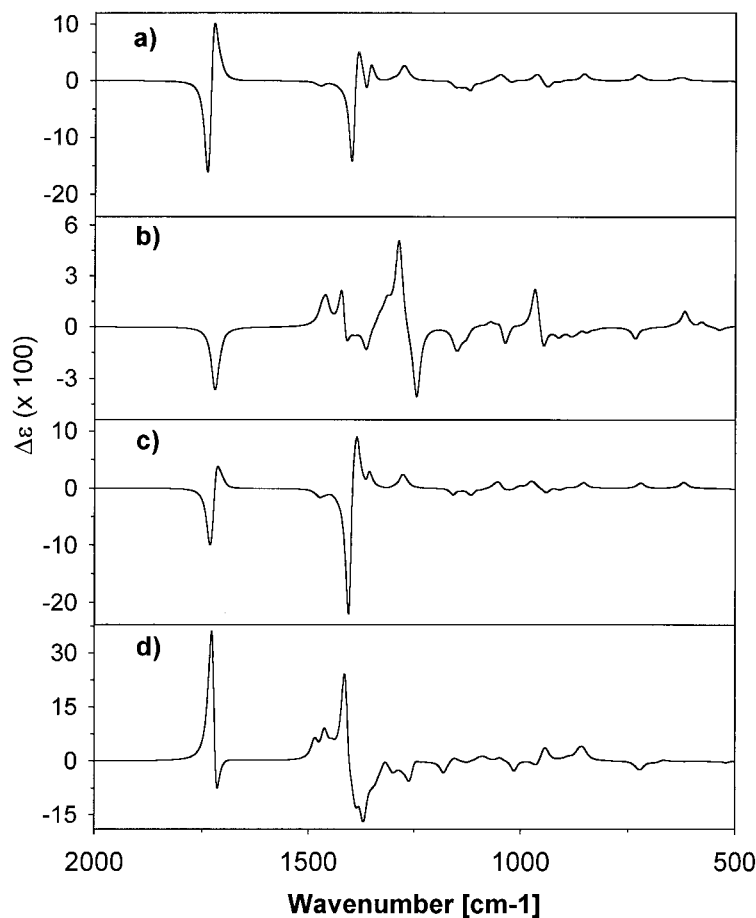


FIGURE 5 Simulated VCD spectrum for the model alanine octapeptide with N—H \rightarrow N—D exchange of the amides in (a) α -helix, (b) β -sheet, (c) 3_{10} -helix, and (d) ProII helix conformations by transferring FF, APT, and AAT tensors from the results for the tripeptide (Figure 1).

the effect of the peptide chain continuation and of the side chains. There is little qualitative change from Figure 3 in the octapeptide spectral patterns for the amide I and amide II vibrations. The α -helix result remains in good agreement with experimental patterns. The β -sheet amide I remains split (though still not enough) and its amide II is now a clear negative couplet (free of interference) yet still weak in intensity, as seen experimentally. The 3_{10} -helix amide I–II relative intensity is improved, as compared to experiment. However, the ProII amide I band shape is worse, becoming too positive, more like the tripeptide (Figure 1) result, but its amide II has very little intensity in agreement with experimental VCD data for coil-like peptides thought to mimic the ProII conformation.^{7,74,77} Larger changes do occur, however, in the lower frequency region involving the amide III vibration, since the CD_3 modes overlap there. Since, for practical reasons, the measurement of protein VCD spectra is mostly restricted to the amide I and II

frequency region and since side chains contribute little to those transitions, these results (Figure 6) are the most generalizable to other sequences.

Site-Specific Carbon 13 Substitution

Spectroscopy of isotopically labeled peptides can dramatically enhance conformational sensitivity of vibrational spectroscopy by giving it a site-selective character that is beyond the normal resolution limitations of ir, Raman or VCD spectroscopy.^{50,55,96,97} The primary effect explored to date is substitution of ^{13}C on the amide C=O which results in a shift of the amide I to lower frequency by $\sim 40\text{ cm}^{-1}$. Extension of this capability to VCD spectra was experimentally demonstrated recently for alanine-rich α -helical oligopeptides labeled with ^{13}C substituted in the carbonyl group.⁹⁸ Theoretical modeling not only aids in reliably interpreting measured VCD data, which is still substantially overlapped, but can also indicate in ad-

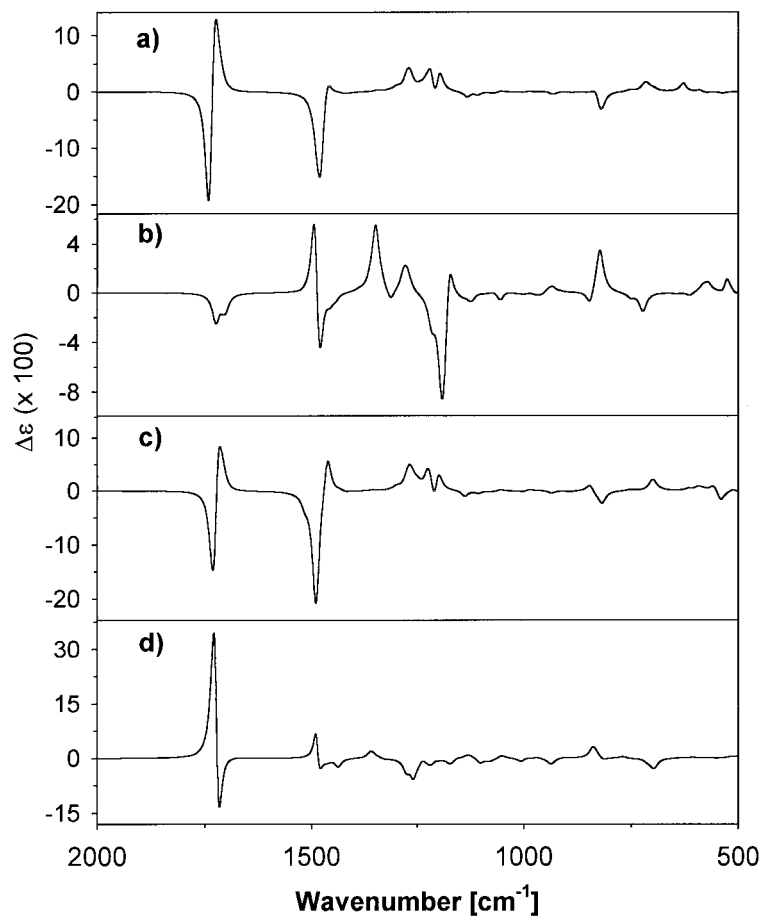


FIGURE 6 Simulated VCD spectrum for the model alanine octapeptide with $\text{CH}_3 \rightarrow \text{CD}_3$ exchange of the alanine side chain in (a) α -helix, (b) β -sheet, (c) 3_{10} -helix, and (d) ProII helix conformations.

vance which would be the most interesting isotopic substitution to study and thus rationalize which syntheses of the labeled species would be most interesting and yield the most structural insight.

Introduction of two ^{13}C labels into various positions of the carbonyl groups of the octapeptide in an α -helical conformation was modeled. Two labels were chosen both to mimic the experiments done⁹⁸ and because our dipeptide VCD simulations had indicated that coupling of two peptides would have conformationally distinctive VCD. The absorption spectra for α -helical octapeptides labeled with an N-terminal, and C-terminal pair of ^{13}C substitutions are shown in Figure 7 (left). The effect of these substitutions can be observed in the amide I region as the appearance of a smaller band shifted by approximately 40 cm^{-1} toward lower frequencies. From comparison with Figure 2a, there is little impact upon the amide II and III modes for these substitutions.

However, the shifts and overall band profiles do depend on the position of the labels in the peptide chain, with the N-terminal label yielding a more resolved shoulder than on the C-terminal, somewhat, as is seen experimentally.⁹⁷ The N-terminal substitution also causes a bigger decrease of the maximum intensity of the amide I band (the ^{12}C contribution), by about 27% as compared to the unsubstituted compound, while the intensity drop for the C-terminal substitution is only 19% (due, in part, to less splitting).

The analogous isotopically labeled simulated VCD spectra are in Figure 7 (right). The ^{13}C spectral side bands have the same shape as the main (^{12}C) feature, a positive couplet, but are more or less resolved depending on the position of the label. Preliminary experimental results for two ^{13}C -labeled residues in a 17-mer indicate that N-terminal labels yield a detectable helical-like side band in VCD but that C-terminal labels do not.⁹⁸ This sort of conservation of the conformation-specific pattern

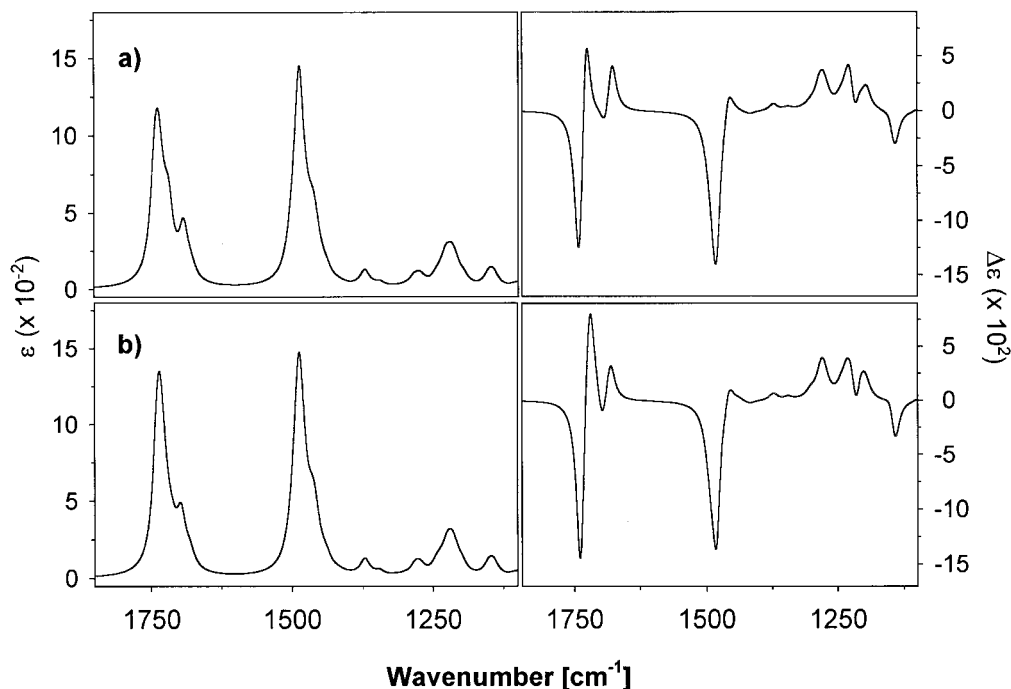


FIGURE 7 Simulated ir absorption (left) and VCD (right) spectrum for the model alanine octapeptide in an α -helical conformation with substitutions at the (a) N-terminal (2,3), and (b) C-terminal (6,7) positions by transferring FF, APT, and AAT parameters from the results for the tripeptide (Figure 1).

under isotopic substitution can be also seen in Figure 8, where simulations of the ir (left) and VCD (right) are compared for four conformations of the octapeptide with the 3,4 positions ^{13}C labeled on the $\text{C}=\text{O}$ of the amide. This substitution was chosen to correspond to the experimentally studied sequence $\text{Ac}-\text{Y}-\text{A}'\text{A}'\text{KAA}-(\text{AAKAA})_2\text{H}-\text{NH}_2$, which is highly α -helical at low temperatures.⁹⁷ The calculated isotopic splitting of 42 cm^{-1} corresponds well to the value of 37 cm^{-1} found experimentally. The predicted decrease of the maximum absorption intensity by 25% corresponds roughly to what has been seen experimentally,⁹⁷ particularly if the differing number of the amide groups in our octapeptide and in the experimental compound (17–20 residues) is taken into account.

From these results we can predict that introduction of such an isotopic probe into a peptide/protein chain will result in the band shape of the VCD spectrum providing unique information about the local conformation at the site-specific location of the probe. By contrast, the shift of the FTIR band does not uniquely specify the conformation due to the various environmental perturbations that can affect frequency. Thus such isotopically site-specific VCD offers the potential of a new structural tool for peptide research.

CONCLUSIONS

VCD band shapes for oligopeptides have been shown to characterize the dominant secondary structure conformational type. These computational results confirm that the major contribution to the VCD band shape is local in nature—primarily due to interactions between nearest neighbor amide groups. Our success at simulating the ir and VCD spectra of the major peptide conformational types is mitigated by two flaws in the simulations. The frequencies, particularly of the amide I, are off by $\sim 100\text{ cm}^{-1}$, more than a minor correction. Preliminary tests suggest that hydrogen-bond formation, while shifting the amide I down and amide II up in frequency, only partially explains the difference of the computed and experimental amide I frequencies. Second, relative amide I and II VCD intensities are off, but this may relate more to APT and FF errors than to the accuracy of the VCD simulation method, since relative amide I and II ir intensities also are off. These latter disagreements are modest and are highly susceptible to features of the model (size of the oligopeptide, transferred couplings, band shape parameters used in the sim-

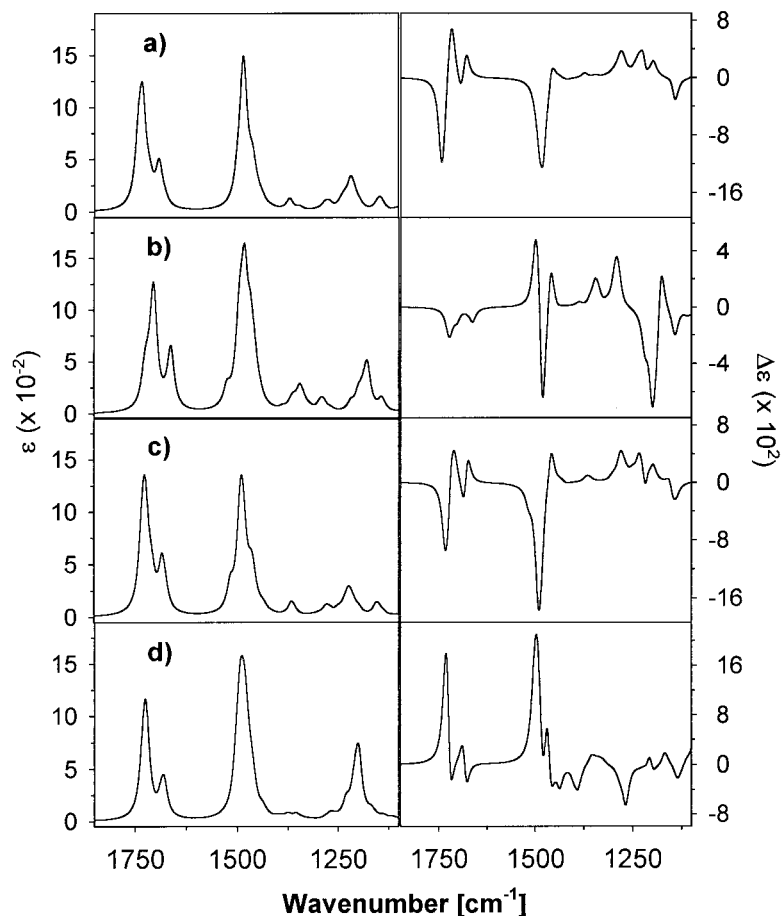


FIGURE 8 Simulated ir absorption (left) and VCD (right) for the model alanine octapeptide with the C=O positions 3,4 (from N-terminal) substituted with ^{13}C in (a) α -helix, (b) β -sheet, (c) 3_{10} -helix, and (d) ProII helix conformations by transferring FF, APT, and AAT from the results for the tripeptide (Figure 1).

ulation). Further development of the computational tools, perhaps by employing ab initio calculations for a larger basis molecule than the tripeptide used here and inclusion of relevant hydrogen bonding, or even transition dipole coupling corrections to the force field, with newer codes and larger computers, then offers the distinct possibility of simulating spectra for polypeptides with multiple conformations. Given control over relative frequencies of the features, perhaps by selectively scaling FF parameters specific for internal coordinates, it is likely that this approach will provide new insight into the deconvolution of ir and VCD band shapes in terms of secondary structure analysis.

Although the nearest-neighbor amide–amide interaction is the dominant, pattern-determining source of the VCD band shape corresponding to a specific conformation, quite a substantial computed contribution for the amide II signal also arises from the amide/side

chain interaction. By contrast, the 1–3 amide–amide interaction does not lead to a change of the basic VCD patterns in the analytically most significant frequency ranges, but results in fine splittings and frequency shifts of spectral bands. This further supports the rationale of transfer of property tensors from oligopeptides to simulate spectra of polypeptides and proteins. The dominance of local interactions furthermore allowed the simulation to be an efficient tool for analysis of VCD of the site-specifically isotopically labeled peptides.

The work was supported by the Grant Agency of the Czech Republic (grant number 203/97/P002 to PB) and in early stages by the NIH (GM30147 to TAK). Computations were performed at the Supercomputer Center in Prague and at the UIC Computer Center. We wish to thank Prof. Sean Decatur, Mt. Holyoke College, for prepublication copies of his work and extensive discussion of the ^{13}C isotope-edited

peptide results. We also wish to thank Prof. Richard Mendelsohn, Rutgers University, for discussion of transition dipole coupling effects on β -sheet amide I ir bands, and the referees for reminding us of Miyazawa's and Krimm's work in this area.

REFERENCES

- Mantsch, H. H.; Chapman, D. *Infrared Spectroscopy of Biomolecules*: Wiley-Liss, Chichester, UK, 1996.
- Surewicz, W. K.; Mantsch, H. H. *Biochem Biophys Acta* 1988, 952, 115–130.
- Byler, D. M.; Susi, H. *Biopolymers* 1986, 25, 469–487.
- Surewicz, W.; Mantsch, H. H.; Chapman, D. *Biochemistry* 1993, 32, 389–394.
- Johnson, W. C., Jr. *Annu Rev Biophys Biophys Chem* 1988, 17, 145–166.
- Johnson, W. C. *Method Enzymol* 1992, 210, 426–447.
- Keiderling, T. A. In *Circular Dichroism and the Conformational Analysis of Biomolecules*; Fasman, G. D., Ed.; Plenum, New York, 1996; pp 555–598.
- Jackson, M.; Mantsch, H. H. *Crit Rev Biochem Mol Biol* 1995, 30, 95–120.
- Pancoska, P.; Wang, L.; Keiderling, T. A. *Protein Sci* 1993, 2, 411–419.
- Martinez, G.; Millhauser, G. *J Struct Biol* 1995, 114, 23–27.
- Jackson, M.; Haris, P. I.; Chapman, D. *Biochim Biophys Acta* 1989, 998, 75–79.
- Yoder, G.; Pancoska, P.; Keiderling, T. A. *Biochemistry* 1997, 36, 15123–15133.
- Williams, S.; Causgrove, T. P.; Gilmanshin, R.; Fang, K. S.; Callender, R. H.; Woodruff, W. H.; Dyer, R. B. *Biochemistry* 1996, 35, 691–697.
- Krimm, S.; Reisdorf, W. C., Jr. *Faraday Disc* 1994, 99, 181–194.
- Torii, H.; Tasumi, M. *J Chem Phys* 1992, 96, 3379–3387.
- Keiderling, T. A. In *Circular Dichroism: Principles and Applications for Chemists and Biologists*, 2nd edition; Nakanishi, K., Berova, N., and Woody, R. A., Eds., John Wiley & Sons, New York, in press.
- Pancoska, P.; Fabian, H.; Yoder, G.; Baumruk, V.; Keiderling, T. A. *Biochemistry* 1996, 35, 13094–13106.
- Pancoska, P.; Keiderling, T. A. *Biochemistry* 1991, 30, 6885–6895.
- Pancoska, P.; Yasui, S. C.; Keiderling, T. A. *Biochemistry* 1989, 28, 5917–5923.
- Yasui, S. C.; Keiderling, T. A. *Biopolymers* 1986, 25, 5–15.
- Malon, P.; Kobrinskaya, R.; Keiderling, T. A. *Biopolymers* 1988, 27, 733–746.
- Baumruk, V.; Huo, D. F.; Dukor, R. K.; Keiderling, T. A.; Lelievre, D.; Brack, A. *Biopolymers* 1994, 34, 1115–1121.
- Baumruk, V.; Keiderling, T. A. *J Am Chem Soc* 1993, 115, 6939–6942.
- Dousseau, F.; Pezolet, M. *Biochemistry* 1990, 29, 8771–8779.
- Lee, D. C.; Haris, P. I.; Chapman, D.; Mitchell, R. C. *Biochemistry* 1990, 29, 9185–9193.
- Pribic, R.; Van Stokkum, I. H. M.; Chapman, D.; Haris, P. T.; Bloemendal, M. *Anal Biochem* 1993, 214, 366–378.
- Johnson, W. C., Jr. *Methods Biochem Anal* 1985, 31, 61–163.
- Sreerama, N.; Woody, R. W. *J Mol Biol* 1994, 242, 497–507.
- Venyaminov, S. Y.; Yang, J. T. In *Circular Dichroism and the Conformational Analysis of Biomolecules*; Fasman, G. D., Ed.; Plenum Press, New York, 1996; pp 69–107.
- Johnson, W. C. *Proteins* 1999, 35, 307–312.
- Pancoska, P.; Bitto, E.; Janota, V.; Urbanova, M.; Gupta, V. P.; Keiderling, T. A. *Protein Sci* 1995, 4, 1384–1401.
- Pancoska, P.; Bitto, E.; Janota, V.; Keiderling, T. A. *Faraday Disc* 1994, 99, 287–310.
- Baumruk, V.; Pancoska, P.; Keiderling, T. A. *J Mol Biol* 1996, 259, 774–791.
- Baello, B. I.; Pancoska, P.; Keiderling, T. A. *Anal Biochem* 1997, 250, 212–221.
- Stephens, P. J.; Lowe, M. A. *Ann Rev Phys Chem* 1985, 36, 213–241.
- Stephens, P. J. *J Phys Chem* 1987, 91, 1712.
- Amos, R. D.; Jalkanen, K. J.; Stephens, P. J. *J Phys Chem* 1988, 92, 5571.
- Jalkanen, K. J.; Stephens, P. J.; Amos, R. D.; Handy, N. C. *J Phys Chem* 1988, 92, 1781.
- Stephens, P. J.; Devlin, F. J.; Ashvar, C. S.; Chabalowski, C. F.; Frisch, M. J. *Faraday Disc* 1994, 99, 103–119.
- Stephens, P. J.; Devlin, F. J.; Chabalowski, C. F.; Frisch, M. J. *J Phys Chem* 1994, 98, 11623–11627.
- Devlin, F. J.; Stephens, P. J. *J Am Chem Soc* 1994, 116, 5003.
- Devlin, F. J.; Finley, J. W.; Stephens, P. J.; Frisch, M. J. *J Phys Chem* 1995, 99, 16883–16902.
- Cheeseman, J. R.; Frisch, M. J.; Devlin, F. J.; Stephens, P. J. *Chem Phys Lett* 1996, 252, 211–220.
- Tam, C. N.; Bour, P.; Keiderling, T. A. *J Am Chem Soc* 1996, 118, 10285–10293.
- Bour, P.; Tam, C. N.; Shaharuzzaman, M.; Chickos, J. S.; Keiderling, T. A. *J Phys Chem* 1996, 100, 15041–15048.
- Ashvar, C. S.; Devlin, F. J.; Stephens, P. J.; Bak, K. L.; Eggimann, T.; Wieser, H. *J Phys Chem* 1998, 102, 6842–6857.
- Ashvar, C. S.; Stephens, P. J.; Eggimann, T.; Wieser, H. *Tetrahedron Asym* 1998, 9, 1107–1110.
- Bour, P.; Keiderling, T. A. *J Am Chem Soc* 1993, 115, 9602–9607.

49. Bour, P.; Sopkova, J.; Bednarova, L.; Malon, P.; Keiderling, T. A. *J Comp Chem* 1997, 18, 646–659.
50. Tadesse, L.; Nazarboghi, R.; Walters, L. *J Am Chem Soc* 1991, 113, 7036–7037.
51. Haris, P. I.; Robillard, G. T.; van Dijk, A. A.; Chapman, D. *Biochemistry* 1992, 31, 6279–6284.
52. Zhang, M. J.; Fabian, H.; Mantsch, H. H.; Vogel, H. J. *Biochemistry* 1994, 33, 10883–10888.
53. Sonar, S.; Liu, X. M.; Lee, C. P.; Coleman, M.; He, Y. W.; Pelletier, S.; Herzfeld, J.; Rajbhandary, U. L.; Rothschild, K. J. *J Am Chem Soc* 1995, 117, 11614–11615.
54. Liu, X. M.; Sonar, S.; Lee, C. P.; Coleman, M.; Rajbhandary, U. L.; Rothschild, K. J. *Biophys Chem* 1995, 56, 63–70.
55. Fabian, H.; Chapman, D.; Mantsch, H. H. In *Infrared Spectroscopy of Biomolecules*; Mantsch, H. H., Chapman, D., Eds.; Wiley-Liss, Chichester, 1996; pp 341–352.
56. Bour, P.; Tam, C. N.; Sopkova, J.; Trouw, F. R. *J Chem Phys* 1998, 108, 351–358.
57. Bour, P. Ph.D. thesis, Academy of Science of the Czech Republic, Prague, Czech Republic, 1993.
58. Kubelka, J. Unpublished results.
59. Jones, R. L. *J Mol Spectrosc* 1963, 11, 411–421.
60. Schweitzer-Stenner, R.; Sieler, G.; Mirkin, N. G.; Krimm, S. *J Phys Chem* 1998, 102, 118–127.
61. Mirkin, N. G.; Krimm, S. *J Mol Struct* 1996, 377, 219–234.
62. Miyazawa, T. *J Chem Phys* 1960, 32, 1647–1652.
63. Krimm, S.; Bandekar, J. *Adv Protein Chem* 1986, 38, 181–364.
64. Krimm, S.; Abe, Y. *Proc Natl Acad Sci USA* 1972, 69, 2788–2792.
65. Moore, W. H.; Krimm, S. *Proc Natl Acad Sci USA* 1975, 72, 4933–4935.
66. Cheam, T. C.; Krimm, S. *Chem Phys Lett* 1984, 107, 613–616.
67. Mendelsohn, R. Personal communication.
68. Lee, S. H.; Krimm, S. *Chem Phys* 1998, 230, 277–295.
69. Creighton, T. E. *Proteins: Structures and Molecular Properties*, 2nd, W. H. Freeman and Co., New York, 1993.
70. Frisch, M. J.; Trucks, G. W.; Schlegel, H. B.; Gill, P. M. W.; Johnson, B. G.; Robb, M. A.; Cheeseman, J. R.; Keith, T.; Petersson, G. A.; Montgomery, J. A.; Raghavachari, K.; Al-Laham, M. A.; Zakrzewski, V. G.; Ortiz, J. V.; Foresman, J. B.; Cioslowski, J.; Stefanov, B. B.; Nanayakkara, A.; Challacombe, M.; Peng, C. Y.; Ayala, P. Y.; Chen, W.; Wong, M. W.; Andres, J. L.; Replogle, E. S.; Gomperts, R.; Martin, R. L.; Fox, D. J.; Binkley, J. S.; Defrees, D. J.; Baker, J.; Stewart, J. P.; Head-Gordon, M.; Gonzalez, C.; Pople, J. A. *Gaussian 94*; Gaussian, Pittsburgh, PA, 1995.
71. Becke, A. D. *J Chem Phys* 1993, 98, 5648–5652.
72. Perdew, J. P.; Wang, Y. *Phys Rev B* 1992, 45, 13244.
73. Amos, R. D. CADPAC: The Cambridge Analytic Derivative Package, Issue 6.0, SERC Laboratory, Daresbury, UK, 1995.
74. Dukor, R. K.; Keiderling, T. A. *Biopolymers* 1991, 31, 1747–1761.
75. Yasui, S. C.; Keiderling, T. A.; Formaggio, F.; Bonora, G. M.; Toniolo, C. *J Am Chem Soc* 1986, 108, 4988–4993.
76. Yoder, G.; Polese, A.; Silva, R. A. G. D.; Formaggio, F.; Crisma, M.; Broxterman, Q. B.; Kamphuis, J.; Toniolo, C.; Keiderling, T. A. *J Am Chem Soc* 1997, 119, 10278–10285.
77. Keiderling, T. A.; Silva, R. A. G. D.; Yoder, G.; Dukor, R. K. *Bioorg Med Chem* 1999, 7, 133–141.
78. LaBrake, C. C.; Wang, L.; Keiderling, T. A.; Fung, L. W. M. *Biochemistry* 1993, 32, 10296–10302.
79. Bour, P.; McCann, J.; Wieser, H. *J Chem Phys* 1998, 108, 8782–8789.
80. Bour, P.; McCann, J.; Wieser, H. *J Phys Chem A* 1998, 102, 102–110.
81. Bour, P.; McCann, J.; Wieser, H. *J Phys Chem A* 1997, 101, 9783–9790.
82. Yang, D.; Rauk, A. J. *J Chem Phys* 1992, 97, 6517.
83. Yasui, S. C.; Keiderling, T. A. *J Am Chem Soc* 1986, 108, 5576–5581.
84. Paterlini, M. G.; Freedman, T. B.; Nafie, L. A. *Biopolymers* 1986, 25, 1751–1765.
85. Yasui, S. C.; Keiderling, T. A.; Bonora, G. M.; Toniolo, C. *Biopolymers* 1986, 25, 79–89.
86. Gupta, V. P.; Keiderling, T. A. *Biopolymers* 1992, 32, 239–248.
87. Sen, A. C.; Keiderling, T. A. *Biopolymers* 1984, 23, 1519–1532.
88. Bour, P. Unpublished.
89. Jalkanen, K. J.; Suhai, S. *Chem Phys* 1996, 208, 81–116.
90. Freedman, T. B.; Nafie, L. A.; Keiderling, T. A. *Biopolymers* 1995, 37, 265–279.
91. Singh, R. D.; Keiderling, T. A. *Biopolymers* 1981, 20, 237–240.
92. Miyazawa, T.; Blout, E. R. *J Am Chem Soc* 1961, 83, 712–719.
93. Miyazawa, T. In *Polyamino Acids, Polypeptides and Proteins: International Symposium*; Stahmann, M. A., Ed.; University of Wisconsin, Madison, WI, 1962; pp 201–217.
94. Narayanan, U.; Keiderling, T. A.; Bonora, G. M.; Toniolo, C. *J Am Chem Soc* 1986, 108, 2431–2437.
95. Pancoska, P.; Yasui, S. C.; Keiderling, T. A. *Biochemistry* 1991, 30, 5089–5103.
96. Braiman, M. S.; Rothschild, K. J. *Annu Rev Biophys Chem* 1988, 17, 541–570.
97. Decatur, S. M.; Antonic, J. *J Am Chem Soc*, 1999, 121, 11914–11915.
98. Silva, R. A. G. D.; Kubelka, J.; Decatur, S. M.; Bour, P.; Keiderling, T. A. To be submitted.